ASCE

Predictive Model for Hurricane Wind Hazard under Changing Climate Conditions

Mirsardar Esmaeili, S.M.ASCE[1]; and Michele Barbato, M.ASCE[2]

Abstract: Hurricanes are among the most destructive and costly extreme weather events. The intensity of future hurricanes is generally expected to increase due to climate change effects. In this work, a simulation method based on a comprehensive statistical analysis of historical data is developed to account for the changes in climatological conditions and their effects on the frequency and intensity of hurricanes. This method is applied to simulate hurricane wind speed distributions under different climatological conditions in the US Atlantic basin from Texas to Maine, which is one of the regions in the world most vulnerable to hurricane hazards. To this end, regression models for several different hurricane parameters are fit to the historical hurricane data. The proposed model is validated by comparing its predicted hurricane-induced wind speeds with available historical data and other existing models based on physics-based hurricane path simulation. This new model is found to reproduce very well historical wind speed distributions and to provide wind speed projection results that are consistent with those of more computationally expensive models based on the simulation of hurricane tracks. The statistical characteristics of future potential hurricanes are simulated using the proposed model along with the climate projections presented in the Fifth Assessment Report of the Intergovernmental Panel for Climate Change. The results of this study indicate that by the year 2060 and depending on the considered projection scenario, the design wind speeds along the US Gulf and Atlantic Coasts corresponding to the different mean return intervals considered by ASCE 7 are expected to increase on average between 14% and 26%, which corresponds to an average increase in the design wind-induced loads of between 30% and 59%. **DOI: 10.1061/(ASCE)NH.1527-6996.0000458.** © *2021 American Society of Civil Engineers.*

Author keywords: Climate change; Hurricane; Hurricane hazard; Sea surface temperature; Wind speed.

Introduction

Tropical cyclones are extreme weather events that often cause extensive social and economic losses worldwide (Huang et al. 2001). The US Gulf and Atlantic Coast regions are frequently struck by these natural events, which are locally referred to as hurricanes. The growing number of resident populations (Crossett et al. 2013) and the concentration of US energy production (Adams et al. 2004) contribute to increasing the hurricane vulnerability of this region. This fact is reflected by the massive losses (normalized to 2017 US dollars) caused by recent hurricanes, e.g., $160 billion losses by Hurricane Katrina in 2005, $125 billion losses by Hurricane Harvey in 2017, and $50 billion losses by Hurricane Irma in 2017 (National Hurricane Center 2018). The observed trend based on 1900–2005 data indicates that hurricane losses in the US Gulf Coast region are doubling every 10 years (Pielke et al. 2008).

The phenomena commonly known as climate change are responsible for changes in the sea water level, sea water temperature, and intensity of extreme weather events, including hurricanes (Stocker et al. 2013). The current consensus among climate scientists is that climate change will very likely produce an intensification of future hurricanes, resulting in potential increases of hurricane-induced losses (Bjarnadottir et al. 2014; Elsner et al. 2011; Hallegatte 2007). By analyzing the data from high-resolution dynamic models, Knutson et al. (2010) concluded that the intensity of hurricanes will increase 2%–11% by 2100 because of global warming. Grinsted et al. (2013) observed that the most extreme weather events are very sensitive to changes in temperature and estimated that the frequency of Katrina-like events could double due to the global warming produced during the 20th century. Significant research has been devoted to modeling the intensification of hurricanes due to climate change (Bjarnadottir et al. 2011, 2014; Emanuel 2011; Knutson et al. 2007, 2013; Emanuel et al. 2008), often based on the climate projection scenarios proposed by the Intergovernmental Panel on Climate Change (IPCC) (Stocker et al. 2013). Some studies approached the problem of estimating future hurricane intensities and corresponding expected induced losses from a statistical point of view based on the abundant available data (Elsner et al. 2011; Jagger et al. 2001; Malmstadt et al. 2010). More recently, hurricane path simulation has been used to predict future hurricane damage to structures and infrastructure systems in a warmer climate. Mudd et al. (2014) developed a framework for assessing climate change effects on the US East Coast hurricane hazards by modeling hurricane paths and decay by combining Georgiou's hurricane wind speed model (Georgiou et al. 1983), an empirical hurricane track model (Vickery et al. 2000), and a hurricane genesis model depending on the sea surface temperature (SST) changes predicted by different climate scenarios (Stocker et al. 2013). Considering the worst-case climate change scenario, they found that the design wind speeds given by ASCE 7-10 for the US Northeast region should be increased by up to 15 m/s for structures of Risk Categories I and II and up to 30 m/s

[1]Ph.D. Student, Dept. of Civil and Environmental Engineering, Univ. of California Davis, One Shields Ave., 2209 Academic Surge, Davis, CA 95616. ORCID: https://orcid.org/0000-0003-1072-8719. Email: mesmaeili@ucdavis.edu

[2]Professor, Dept. of Civil and Environmental Engineering, Univ. of California Davis, One Shields Ave., 3149 Ghausi Hall, Davis, CA 95616 (corresponding author). ORCID: https://orcid.org/0000-0003-0484-8191. Email: mbarbato@ucdavis.edu

Note. This manuscript was submitted on July 16, 2020; approved on November 18, 2020; published online on March 27, 2021. Discussion period open until August 27, 2021; separate discussions must be submitted for individual papers. This paper is part of the ***Natural Hazards Review***, © ASCE, ISSN 1527-6988.

for structures of Risk Categories III and IV to ensure that structures designed today will achieve appropriate target safety and expected performance levels in the year 2100 (Mudd et al. 2014). Cui and Caracoglia (2016) developed a framework for estimating the lifetime costs of tall buildings subject to hurricane-induced damage under different climate change scenarios by means of a statistical hurricane track path model. Under the worst-case scenario, they estimated that the hurricane-induced losses on tall buildings could increase up to 30% from 2015 to 2115. Lee and Ellingwood (2017) developed a framework for risk assessment of infrastructures with long expected service periods accounting for the effects of climate change by adopting the model of Vickery et al. (2000). Pant and Cha (2018) developed a framework to account for the effects of climate change on hurricane wind–induced damage and losses for residential buildings in Miami-Dade County, Florida. They used Georgiou's model (Georgiou et al. 1983) in conjunction with a transition matrix to simulate the hurricane track and developed relationships between average yearly SST and hurricane parameters used for hurricane genesis. They found that for each 1°C increase, the 3-s average wind speed for a 700-year return period is expected to increase by about 6.7–8.9 m/s for the county, and the accumulated hurricane-induced losses in the 2016–2055 period are expected to increase by 1.4–1.7 times the expected losses predicted for the 2006 climatological conditions.

Climate change affects all hazards associated with hurricane events, i.e., wind, windborne debris, storm surge, and rain hazards (Barbato et al. 2013; Unnikrishnan and Barbato 2017). This paper focuses only on hurricane wind hazard. The objective is to develop an accurate and efficient statistical model for wind hazard in coastal areas that can account for the nonstationary climatological conditions produced by climate change. A simulation procedure based on an indirect statistics approach is proposed in this study.

This paper is organized as follows: (1) the vector of parameters necessary to describe the hurricane wind hazard, referred to as an intensity measure (IM) vector, is identified and a statistical model is developed for its components as functions of climatological conditions, synthetically described by SST; (2) using a multilayer Monte Carlo simulation approach and an existing hurricane wind profile model, a wind distribution simulation procedure for coastal sites and given SST is developed; (3) the model simulation capabilities are validated through a comparison with historical data from the National Institute of Standards and Technology (NIST 2016) and the design wind speeds from ASCE 7-16 (ASCE 2016); and (4) the results of the developed simulation approach are compared with those of other existing models based on the simulation of hurricane tracks, i.e., the models developed by Cui and Caracoglia (2016) and Pant and Cha (2019), and the proposed model is used to develop hurricane wind speed distributions along the US Gulf and Atlantic Coasts based on the climate scenarios presented in the IPCC Fifth Assessment Report (AR5) (Stocker et al. 2013).

Research Significance

This research proposes a predictive simulation approach to quantify the nonstationary effects of climate change on hurricane wind speeds along the US Gulf and Atlantic Coasts. This simulation procedure innovatively uses a simple and efficient indirect statistics approach (Unnikrishnan and Barbato 2017), in which the statistics of the different IMs are indirectly obtained from site-specific statistics of fundamental hurricane parameters. The major contribution of this method is the lower computational cost compared to full track approaches found in the literature (Cui and Caracoglia 2016; Lee and Ellingwood 2017; Mudd et al. 2014; Pant and Cha 2018, 2019), which can allow researchers and practicing engineers to consider a significantly higher number of scenarios at only a fraction of the computational cost of a single scenario for a full track approach. The proposed methodology is specialized in this paper for the US Gulf and Atlantic Coasts; however, it can be easily extended to other regions worldwide by using appropriate statistical data from pertinent historical records.

Modeling IMs as Functions of SST

This study uses the SST at the location and time of a given hurricane, T, as the main indicator of climate change effects on hurricane properties. This selection is consistent with the high correlation between hurricane intensity and SST (Bjarnadottir et al. 2011; Elsner et al. 2012; Emanuel 2011, 1999; Vickery et al. 2000, 2009; Webster et al. 2005), explained by the increase in warm water evaporation that fuels hurricanes as SST increases. Consistently with an indirect statistics approach, the following subset of IM components were selected as the primary IMs affected by climate change: hurricane annual frequency, ν_h; peak hurricane wind speed (here defined as the maximum 1-min average speed measured at a height of 10 m over open terrain), V_{max}; radius to maximum wind speed, R_{max}; and translational wind speed, V_t. These IM components were selected because they are consistent with the hurricane radial wind profile model proposed by Willoughby et al. (2006) to describe the pressure gradient component, $V_r(r)$, of hurricane wind speed at a given distance, r, from the hurricane eye.

All IMs except ν_h are modeled as functions of T to account for the nonstationary climatic conditions produced by climate change. In particular, means and standard deviations are defined by a linear regression model whose parameters are based on historical data, as follows:

$$\mu_p(T) = a_{p0} + a_{p1} \cdot T \tag{1}$$

$$\sigma_p(T) = b_{p0} + b_{p1} \cdot T \tag{2}$$

in which $p = V_{max}$, R_{max}, V_t. For each IM, a modified Kolmogorov-Smirnov statistical test (Soong 2004) was used to identify an appropriate probability distribution. Note that this approach is different from that adopted in Pant and Cha (2018), in which the linear regression models of the hurricane parameters were developed as functions of the average yearly SST, T_y.

Hurricane Frequency Model

Current literature indicates a significant level of disagreement among different researchers regarding the variation in hurricane frequency and the development of an appropriate hurricane frequency model under changing climate conditions (Lombardo and Ayyub 2015). In this work, climate change–induced modifications of the hurricane annual frequency were investigated by analyzing the yearly number of hurricanes, n_h, in the US Gulf and Atlantic Coasts during the 1851–2018 period as a function of the yearly global T_y, plotted in Fig. 1(a) based on the hurricane records in the HURDAT2 database (Landsea et al. 2015). The slope of the linear regression model used to fit the historical data is almost equal to zero, i.e., the annual frequency for Atlantic hurricanes is independent of T_y (p-value = 0.95). The same methodology was followed to investigate climate change effects on the hurricane annual frequency at different marine mileposts at intervals of 185.2 km (100 nautical miles) along the US Gulf and Atlantic Coast regions [shown in Fig. 1(b)], based on the hurricane annual frequencies given in the NIST database (NIST 2016). For all considered mileposts,

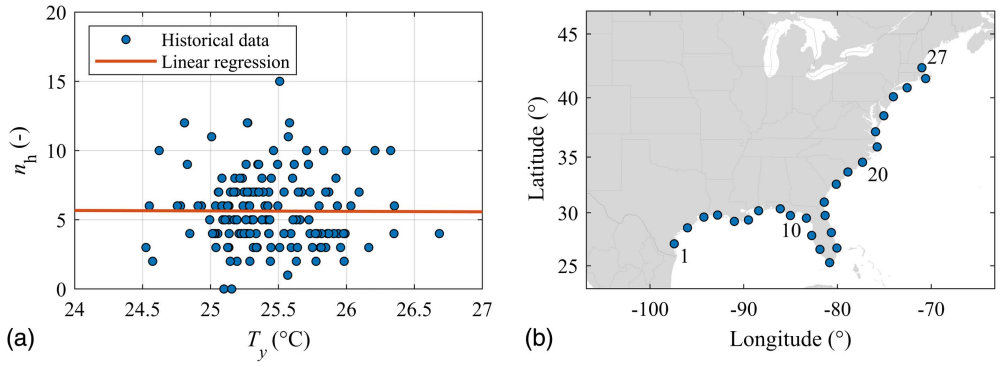

Fig. 1. US Gulf and Atlantic coast hurricane-prone region: (a) yearly number of hurricanes in 1851–2018 period as function of T_y; and (b) location of mileposts at intervals of 185.2 km (100 nautical miles) considered in this study.

the slope of the linear regression was found to be statistically equal to zero, with p-values ranging between 0.74 and 0.86. Based on the existing literature, two distributions were considered to model the hurricane annual occurrences: the Poisson distribution (Batts et al. 1980; Mudd et al. 2014) and the negative binomial distribution (Cui and Caracoglia 2016; Jagger and Elsner 2012; Oxenyuk et al. 2017; Vickery et al. 2000). A χ^2 goodness-of-fit test (Soong 2004) failed to reject the null hypothesis at a 5% significance level in 24 of 27 locations for the Poisson distribution (i.e., the fitting of the available data with a Poisson distribution was acceptable for 24 of 27 locations) and in 10 of 27 locations for the negative binomial distribution (i.e., the fitting of the available data with a negative binomial distribution was acceptable for 10 of 27 locations). It was also observed that for the 17 locations where the negative binomial distribution was rejected, the sample mean of the number of annual hurricanes was higher than the corresponding sample variance, confirming that the use of a negative binomial distribution was not appropriate for those locations.

Based on these results, the yearly number of hurricanes affecting a given location is modeled as a Poisson random variable with constant (i.e., not dependent on T_y) annual frequency, ν_h, equal at each location to the annual hurricane frequency given in the NIST database (NIST 2016). The values of ν_h corresponding to the considered mileposts along the US Gulf and Atlantic Coasts are given in Table 1.

Model for SST at Time and Location of Hurricane

This study proposes a model for the SST at the place and location of a hurricane, T, as a function of climatic conditions, which are synthetically represented by the average yearly SST, T_y. The SST T is assumed to follow a probability distribution with mean and standard deviation described as linear functions of T_y. The linear regression models were developed using the National Oceanic and Atmospheric Administration (NOAA) data sets for T and T_y corresponding to the period 1988–2018 (NOAA/OAR/ESRL-PSD 2015). The obtained relation for the mean SST, μ_T, is plotted in Fig. 2(a) with the historical data and is given by

$$\mu_T(T_y) = a_{T0} + a_{T1} \cdot T_y \tag{3}$$

in which $a_{T0} = -27.38$°C and $a_{T1} = 2.19$. Eq. (3) is valid for $T_y \geq 24.0$°C. The standard deviation was found to be almost independent of T_y, with the slope of the regression line statistically equal to zero (p-value = 0.33). Thus, the SST standard deviation is assumed constant and equal to $\sigma_T = 1.23$°C. Based on the results of a modified Kolmogorov-Smirnov test (Soong 2004), a normal distribution with mean given by Eq. (3) and $\sigma_T = 1.23$°C is selected to describe T.

Peak Wind Speed Model

A statistical model for V_{max} as a function of T was developed based on the historical peak hurricane wind speeds collected from the HURDAT2 database (Landsea et al. 2015) and the maximum temperature at the time and location of a hurricane obtained from the NOAA database (NOAA/OAR/ESRL-PSD 2015) for hurricanes in the Atlantic basin during the period 1988–2018. The historical data of V_{max} are plotted as a function of T in Fig. 2(b) together with the linear regression model used to describe $\mu_{V_{max}}(T)$. The regression parameters for the mean and standard deviation of V_{max} according

Table 1. Location-dependent parameters for mileposts at intervals of 185.2 km (100 nautical miles) along US Gulf and Atlantic coasts

Milepost number	ν_h	r_{inf} (km)	λ (km)	κ (km)	ξ
1	0.37	275	215	39.96	−0.71
2	0.44	285	208	41.74	−0.10
3	0.48	270	212	39.13	−0.75
4	0.51	295	223	43.66	−0.36
5	0.50	290	225	42.67	−0.60
6	0.50	295	230	43.56	−0.67
7	0.50	285	220	41.83	−0.56
8	0.51	285	225	41.73	−0.83
9	0.50	295	230	43.96	−0.87
10	0.51	295	235	43.76	−0.92
11	0.51	290	229	37.58	−0.87
12	0.53	225	178	30.99	−0.84
13	0.57	255	192	42.29	−0.40
14	0.55	215	171	42.03	−1.04
15	0.63	300	224	54.67	−0.37
16	0.57	345	268	62.58	−0.69
17	0.53	345	274	62.53	−0.98
18	0.55	320	252	58.66	−0.74
19	0.61	280	221	51.57	−0.46
20	0.68	285	225	51.44	−0.89
21	0.63	268	212	48.29	−0.17
22	0.56	297	234	54.33	−0.65
23	0.45	325	257	58.53	−0.26
24	0.32	307	243	55.48	−0.84
25	0.29	270	213	48.93	−1.01
26	0.29	270	214	48.96	−0.79
27	0.26	292	231	52.85	−0.45

Note: ν_h = hurricane annual frequency; r_{inf} = radius of influence; λ = location parameter; κ = scale parameter; and ξ = shape parameter.

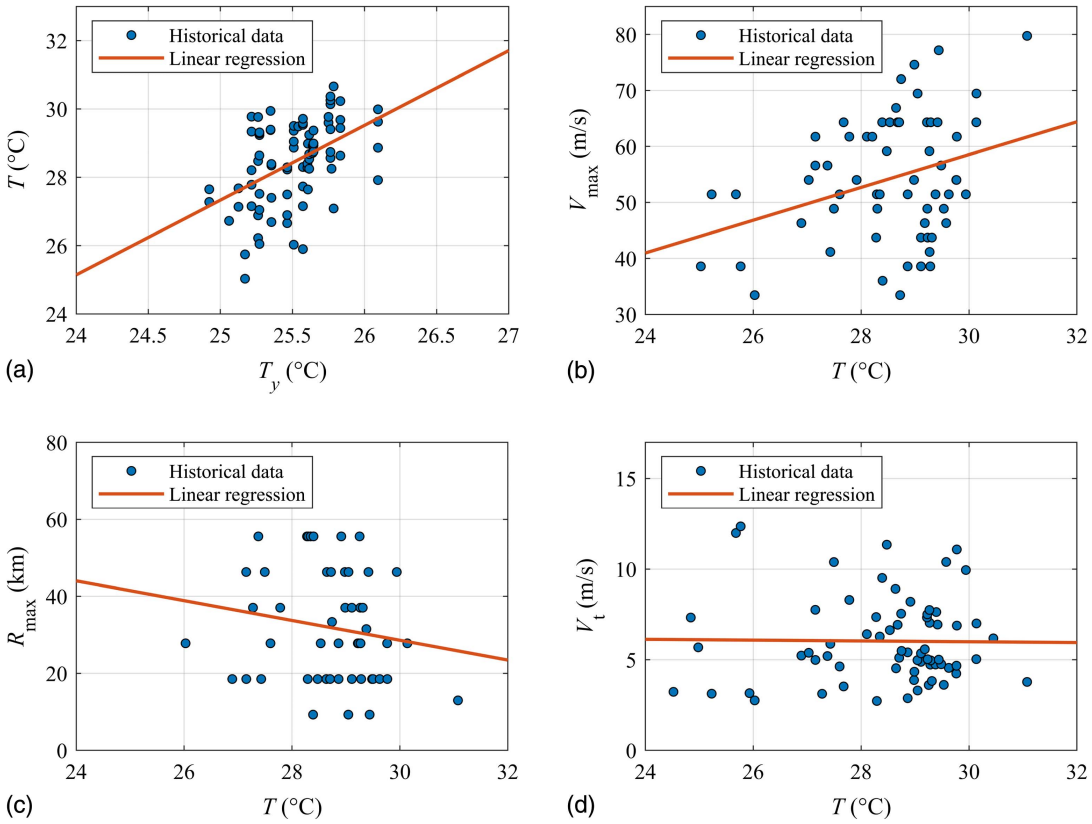

Fig. 2. Historical data for US Gulf and Atlantic coasts in period 1988–2018 and linear regression lines for (a) T versus T_y; (b) V_{max} versus T; (c) R_{max} versus T; and (d) V_t versus T.

to Eqs. (1) and (2) (as well as the p-values of the slopes of the regressions) are given in Table 2 and are valid for $T \geq 24$°C. Based on the results of a two-sided Kolmogorov-Smirnov test (Soong 2004), the Weibull distribution provides the best fit to the collected data and is adopted here, consistent with other research works available in the literature (e.g., Li and Ellingwood 2006).

Radius to Maximum Wind Speed Model

The statistical model for R_{max} was developed using the same approach and the same data sources used for V_{max}. The historical data of R_{max} are plotted as a function of T in Fig. 2(c) together with the linear regression model used to describe $\mu_{R_{max}}(T)$. The regression parameters for the mean and standard deviation of R_{max} according to Eqs. (1) and (2) (as well as the p-values of the slopes of the regressions) are given in Table 2 and are valid for $T \geq 24$°C. Based on the results of a two-sided Kolmogorov-Smirnov test (Soong 2004), the truncated normal distribution with lower tail truncation $R_{max} > 0$ provides the best fit to the collected data and is adopted here, consistent with other research works available in the literature (Bjarnadottir et al. 2011; Unnikrishnan and Barbato 2017). A weak but nonnegligible inverse correlation between V_{max} and R_{max} was also found, with a correlation coefficient $\rho_{V_{max}R_{max}} = -0.301$.

Translational Wind Speed Model

A statistical model for V_t was developed following a similar approach and the same data sources used for V_{max} and R_{max}. Because the values of V_t are not directly available in the HURDAT2 database (Landsea et al. 2015), they were calculated as the maximum values of the translational speed along each hurricane track by assuming a constant translational speed between subsequent recorded positions of the tropical cyclone center. Fig. 2(d) shows the historical data for V_t and the linear regression fit for the mean of V_t as a function of T. The slopes of the linear regressions for the mean and standard deviation of V_t are not statistically different than zero (Table 2); thus, both the mean and standard deviation of V_t are assumed to be independent of T. Based on the results of a two-sided Kolmogorov-Smirnov test (Soong 2004), a log-normal distribution with $\mu_{V_t} = 6.02$ m/s and $\sigma_{V_t} = 2.45$ m/s provides the best fit to the collected data and is adopted here. It is noteworthy that V_t is a variable that is location-dependent, with hurricanes generally

Table 2. Regression parameters for mean and standard deviation of hurricane IMs for US Gulf and Atlantic coasts

p	Unit	a_{p0}	$a_{p1} \cdot$ °C	p-value	b_{p0}	$b_{p1} \cdot$ °C	p-value
V_{max}	m/s	−29.31	2.93	0.01	−20.05	1.06	<0.01
R_{max}	km	105.8	−2.57	0.05	29.0	−0.48	<0.01
V_t	m/s	6.66 (6.02)[a]	−0.02 (0)[a]	0.91	−3.52 (2.45)[a]	0.21 (0)[a]	0.37

[a]Values in parentheses are those used in the proposed sampling procedure.

- Select the site of interest by setting: latitude, longitude, ν_h, and r_{inf}.
- Select the number of samples: n_s.
- Select the year of interest: y.
- For $i = 1 : n_s$
  - If $y \le 2005$:
    - Set $T_y^{(i)}$ equal to historical value corresponding to year y.
  - Else
    - Select projection scenario.
    - Sample $\Delta T_y^{(i)}$ from a normal distribution based on IPCC AR5 projections.
    - Calculate $T_y^{(i)}$ from Eq. (4).
  - End if.
  - Sample number of yearly hurricanes, $n_h^{(i)}$, from a Poisson distribution with event rate = ν_h.
  - If $n_h^{(i)} = 0$:
    - Set: $V^{(i)} = 0$ m/s
  - Else
    - For $j = 1 : n_h^{(i)}$
      - Sample the hurricane eye location, i.e., bearing angle $\theta^{(i,j)}$, and distance $r^{(i,j)}$ using the distributions given in Table 3. If hurricane eye location is on land, resample until hurricane eye location is on water.
      - Calculate $\mu_T\left(T_y^{(i)}\right)$ from Eq. (3) and sample $T^{(i,j)}$.
      - Calculate $\mu_{V_{max}}\left(T^{(i,j)}\right)$ and $\mu_{R_{max}}\left(T^{(i,j)}\right)$ from Eq. (1), and $\sigma_{V_{max}}\left(T^{(i,j)}\right)$ and $\sigma_{R_{max}}\left(T^{(i,j)}\right)$ from Eq. (2). Set $\mu_{V_t} = 6.02$ m/s and $\sigma_{V_t} = 2.45$m/s.
      - Sample $V_{max}^{(i,j)}$, $R_{max}^{(i,j)}$, and $V_t^{(i,j)}$ from the distributions given in Table 3.
      - Sample $A^{(i,j)}$, $n^{(i,j)}$, and $X_1^{(i,j)}$ using a Nataf's model based on the probability distributions given in Table 3.
      - Calculate $V_r^{(i,j)}$ from Eq. (5).
      - Sample $\beta^{(i,j)}$ from the distribution given in Table 3 and calculate $\alpha^{(i,j)}$.
      - Calculate $V^{(i,j)}$ at the site from Eq. (6).
  - End if

End for

Fig. 3. Flowchart of proposed hurricane wind speed simulation methodology.

moving faster north along the Atlantic Coast region and moving slower inside the Gulf Coast region (Vickery et al. 2009, 2000). However, a single random variable is used here to describe the hurricane translation wind speed over the entire US Gulf and Atlantic Coast region. In fact, this quantity has a small effect on peak wind speeds, which represent the focus of this study. This modeling assumption is not appropriate when modeling other hazards, such as storm surge and rainfall, which are strongly dependent on the translational wind speed of tropical cyclones. For these applications, it is recommended to use multiple location-dependent random variables to describe V_t.

Development of Hurricane Wind Speed Distributions for US Gulf and Atlantic Coasts as Function of Climatological Conditions

A simulation approach based on a multilayer Monte Carlo simulation (Barbato et al. 2013; Unnikrishnan and Barbato 2017) is proposed here to develop hurricane wind speed distributions at different locations as functions of climatological conditions described by changes in the SST. A flowchart of the simulation algorithm is provided in Fig. 3. The random parameters used in the sampling procedure and their probability distributions are described in Table 3.

The methodology is initialized by selecting the location (latitude and longitude) of the site of interest, the number of samples, n_s, and the year of interest, y. Once the location is selected, the corresponding value of ν_h is obtained from the NIST database (NIST 2016). The sampling procedure starts by finding the average yearly SST, $T_y^{(i)}$, for sample i. If the simulation is done to validate historical data (in this study, when $y \le 2005$), $T_y^{(i)}$ is set deterministically equal to the measured average yearly SST for the year under consideration, e.g., using data from NOAA's records (NOAA/OAR/ESRL-PSD 2015). If the simulation is performed to predict future wind speed distributions for a given scenario, the temperature increment $\Delta T_y^{(i)}$ is sampled based on the data reported in the IPCC AR5 (Stocker et al. 2013). These data correspond to the mean and the 90% confidence intervals for the predicted global annual SST changes in the 2010–2060 period with respect to 2005, which are reported in Fig. 4. In particular, the filled markers represent the mean estimates, whereas the empty markers correspond to the lower and upper bounds of the 90% confidence intervals. This figure also shows the estimated global annual SST change for 2010 and 2015 with respect to 2005. The lower and upper bounds of the 90% confidence

Table 3. Random variables and corresponding probability distributions used in proposed sampling procedure

Variable	Unit	Distribution	Distribution description	Range
ΔT_y	°C	Truncated normal	Based on IPCC AR5 (Stocker et al. 2013) projections	$-1.73 \le \Delta T_y \le +\infty$
n_h	—	Poisson	ν_h at each location from NIST database (2016)	$n_h \ge 0$
θ	rad	Uniform	$\mu_\theta = \pi$, $\sigma_\theta = \pi^2/3$	$0 \le \theta \le 2\pi$
R	km	tGEV	Parameters $r_{inf}, \lambda, \kappa, \xi$ at each location given in Table 1	$0.0 \le r \le r_{inf}$
T	°C	Truncated normal	μ_T calculated from Eq. (3), $\sigma_T = 1.23$°C	$T \ge 24$°C
V_{max}	m/s	Translated weibull	$\mu_{V_{max}}$ calculated from Eq. (1), $\sigma_{V_{max}}$ calculated from Eq. (2)	$V_{max} \ge 33.4$ m/s
R_{max}	km	Truncated normal	$\mu_{R_{max}}$ calculated from Eq. (1), $\sigma_{R_{max}}$ calculated from Eq. (2)	$R_{max} \ge 0.0$ km
V_t	m/s	Lognormal	$\mu_{V_t} = 6.02$ m/s, $\sigma_{V_t} = 2.45$ m/s	$V_t \ge 0.0$ m/s
A	—	Mixed GEV	$0.61 + 0.39 \cdot$ tGEV(ξ, κ, λ)	$0.0 \le A \le 1.0$
			$\xi = 0.1392$, $\kappa = 0.1517$, $\lambda = 0.2044$	
X_1	km	Weighted GEV	$\xi_1 = -0.0023$, $\kappa_1 = 65.40$, $\lambda_1 = 210.55$	$100 \le X_1 \le 500$ km
			$\xi_2 = 0.6519$, $\kappa_2 = 2.4885$, $\lambda_2 = 452.41$	
n	—	Truncated lognormal	$\mu_n = 0.8808$, $\sigma_n = 0.4252$	$0.0 \le n \le 2.5$
β	rad	Normal	From Vickery et al. (2000)	$0 \le \beta \le 2\pi$

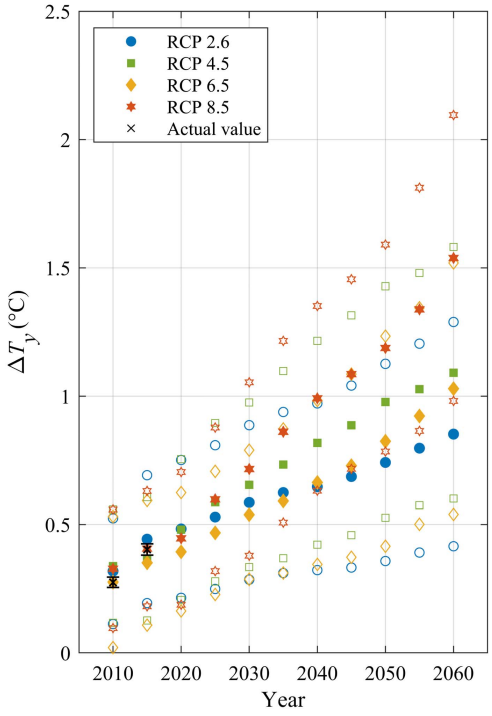

Fig. 4. IPCC AR5 projections for increases in average yearly sea surface temperature.

intervals for the measured ΔT_y in 2010 and 2015 are not visible at the scale used in Fig. 4 and are equal to [0.25, 0.29]°C for 2010 and [0.38, 0.42]°C for 2015. The IPCC AR5 projections do not provide the probability distribution for the average yearly SST increase. In the present study, the average yearly SST change in any given year is assumed to follow a truncated normal distribution (with the lower bound equal to −1.73°C) fitted to data corresponding to the different IPCC AR5 projections (Stocker et al. 2013). The ith sample value of T_y for the year and scenario of interest is finally obtained as

$$T_y^{(i)} = T_{2005} + \Delta T_y^{(i)} \tag{4}$$

in which $T_{2005} = 25.73$°C is the average yearly SST for the reference year 2005 used by the IPCC AR5 projection scenarios. The lower bound of the ΔT_y distribution was selected so that $T_y \ge 24$°C, consistent with the validity range for Eq. (3).

The next step of the sampling procedure requires sampling the number of hurricanes in a year for the ith sample, $n_h^{(i)}$, from a Poisson distribution with an event rate equal to ν_h for the location of interest. If $n_h^{(i)} = 0$, then the yearly maximum wind speed for the ith sample is set equal to zero, i.e., $V^{(i)} = 0$ m/s. Otherwise, an inner loop is initiated to obtain the maximum wind speeds for each of the sampled hurricanes in a year corresponding to the ith sample.

For the jth hurricane of this inner loop [where $j = 1, 2, \ldots, n_h^{(i)}$], the sampling procedure requires sampling the position of the hurricane eye closest to the location of interest, conditional on this position being on water. More specifically, a bearing angle, $\theta^{(i,j)}$, and a distance, $r^{(i,j)}$, are sampled from a uniform distribution and a truncated generalized extreme value distribution (tGEV), respectively, as described in Table 3. The values of the parameters defining the tGEV distribution (i.e., radius of influence r_{inf}, location parameter λ, scale parameter κ, and shape parameter ξ) are given in Table 1 for the different locations considered in this study [Fig. 1(b)]. The values of r_{inf} were calculated using historical hurricane tracks for mileposts along the US Gulf and Atlantic Coasts at intervals of 185.2 km (100 nautical miles) using the HURDAT2 database (Landsea et al. 2015) and considering all the hurricanes in the Atlantic basin during the period 1871–1963, i.e., the period for which the NIST database was developed (Batts et al. 1980). In particular, the values of r_{inf} were obtained by rounding to the next 10 km the distance within which the hurricane frequency obtained from the historical data coincides with the hurricane annual frequency provided by the NIST database, ν_h. The values of the other parameters were obtained by fitting a tGEV distribution to the historical data from the HURDAT2 database (Landsea et al. 2015). Only hurricane location samples positioned on water are accepted by digitizing the map of the region and rejecting the location samples on land until the condition is satisfied. The procedure to identify the hurricane eye's position from the latitude and longitude of the site of interest and the sampled values of r and θ is described in Todhunter (2006).

Once the hurricane eye's position is determined, the temperature $T^{(i,j)}$ at the time and location of the hurricane is sampled from a truncated normal distribution with lower limit equal to 24°C, mean $\mu_T(T_y^{(i)})$ obtained from Eq. (3), and standard deviation $\sigma_T = 1.23$°C. The probability distributions shown in Table 3 are used in combination with Nataf's model (Liu and Der Kiureghian 1986) to sample the remaining IM components $V_{max}^{(i,j)}$, $R_{max}^{(i,j)}$, and $V_t^{(i,j)}$, with correlation coefficients $\rho_{R_{max},V_{max}} = -0.301$ and $\rho_{V_{max},V_t} = \rho_{R_{max},V_t} = 0$. The parameter values given in Table 2 are used in

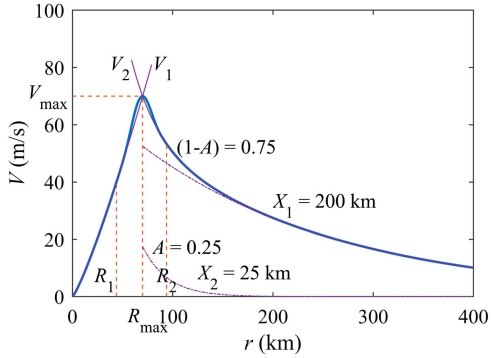

Fig. 5. Description of Willoughby's hurricane profile model.

conjunction with Eq. (1) to determine $\mu_{V_{\max}}(T^{(i,j)})$ and $\mu_{R_{\max}}(T^{(i,j)})$, and with Eq. (2) to determine to determine $\sigma_{V_{\max}}(T^{(i,j)})$ and $\sigma_{R_{\max}}(T^{(i,j)})$.

The next step of the sampling procedure requires calculating the pressure gradient component of the wind speed, $V_{\mathrm{r}}^{(i,j)}$, which in this study is based on Willoughby's model for a dual-exponential hurricane profile (Willoughby et al. 2006). This model is a piecewise continuous profile for the pressure gradient component of hurricane wind speed defined as follows (Fig. 5):

$$V_{\mathrm{r}}(r)=\begin{cases} V_1=V_{\max}\cdot\left(\dfrac{r}{R_{\max}}\right)^n & 0\le r\le R_1 \\ V_1\cdot(1-w)+V_2\cdot w & R_1<r<R_2 \\ V_2=V_{\max}\cdot\left[(1-A)\cdot e^{\left(-\frac{r-R_{\max}}{X_1}\right)}+A\cdot e^{\left(-\frac{r-R_{\max}}{X_2}\right)}\right] & r\ge R_2 \end{cases} \tag{5}$$

where n is the exponent controlling the wind speed increase inside the hurricane eye; w denotes a weighting function described by a smooth ninth-order polynomial that monotonically increases from zero to one in the transition zone defined by $R_1 \le R_{\max} \le R_2$; X_1 and X_2 denote the e-folding lengths; and A is a parameter determining the proportion of the two exponentials in the profile outside the transition zone. Based on Willoughby et al. (2006), $R_2 = R_1 + 10$ km, $X_2 = 25$ km, whereas n, X_1, and A are correlated random variables described by the probability distributions given in Table 3 with correlation coefficients $\rho_{X_1 n} = -0.143$, $\rho_{X_1 A} = 0.165$, and $\rho_{nA} = 0.391$. These distributions were obtained by fitting to the data provided for the dual-exponential model in Willoughby et al. (2006). Also in this case, statistical sampling of the correlated random variables n, X_1, and A is performed using Nataf's model (Liu and Der Kiureghian 1986). The parameter R_1 is a function of n, A, X_1, X_2, and $R_{\max}$ and is found by numerical inversion of the ninth-order polynomial defining w after calculating the value of w corresponding to $V_{\max}$ (Willoughby et al. 2006).

Finally, the heading angle $\beta^{(i,j)}$ is sampled from a normal distribution with mean and standard deviation derived from historical data (Vickery et al. 2000). Using Georgiou's model (Georgiou et al. 1983), the sampled pressure gradient and translational wind speeds, $V_{\mathrm{r}}^{(i,j)}$ and $V_{\mathrm{t}}^{(i,j)}$, are combined to obtain the maximum gradient wind speed at the site of interest, $V^{(i,j)}$

$$V^{(i,j)} = \frac{1}{2}\cdot\left[V_{\mathrm{t}}^{(i,j)}\cdot\sin(\alpha^{(i,j)}) - f\cdot r^{(i,j)}\right] + \sqrt{\frac{1}{4}\cdot\left[V_{\mathrm{t}}^{(i,j)}\cdot\sin(\alpha^{(i,j)}) - f\cdot r^{(i,j)}\right]^2 + \left(V_{\mathrm{r}}^{(i,j)}\right)^2} \tag{6}$$

in which $\alpha^{(i,j)}$ is the relative angle between the translational direction of the hurricane [defined by the heading angle $\beta^{(i,j)}$] and the direction defined by connecting the site of interest with the hurricane eye position; and f is the Coriolis parameter.

The simulated hurricane wind speeds obtained using the proposed sampling procedure can then be postprocessed depending on the statistics of interest. For example, if the statistic of interest is the annual peak wind speed distribution at the site, the experimental cumulative distribution function (CDF) can be obtained using only the yearly maxima, i.e., $V^{(i)} = \max_{1\le j\le n_h^{(i)}}(V^{(i,j)})$. Note also that the hurricane wind speed obtained from the proposed sampling procedure corresponds to the fastest 1-min hurricane speed at 10 m above ground over open terrain, i.e., equivalent to Exposure Category C in ASCE 7-16 (ASCE 2016). The simulated hurricane wind speeds V can then be converted to different gust averaging times, exposures, and elevations as follows:

$$V_{t,e,z} = c_t \cdot c_e \cdot c_z \cdot V \tag{7}$$

where c_t = conversion factor for different wind time averages (ESDU 1993; ASCE 2016), with $c_t = 1$ for the fastest 1-min hurricane speed; c_e = conversion factor for different terrain exposure categories (ASCE 2016), with $c_e = 1$ over open terrain (Exposure Category C); and c_z = conversion factor for different elevations z above ground (ASCE 2016), with $c_z = 1$ at $z = 10$ m above ground.

Validation of Proposed Model with Historical Data

The proposed simulation procedure for the hurricane wind speed at a given location along the US Gulf and Atlantic Coasts is validated by comparing the statistics of the simulation results with two sets of historical data: hurricane wind speeds from the NIST database (NIST 2016) and design wind speeds from ASCE 7-16 (ASCE 2016). The first set of data from the NIST database (NIST 2016) is used to validate the means and the standard deviations (i.e., the body region of the corresponding distribution) of historical hurricane wind speeds during the 1871–1963 period for the considered mileposts. The simulation procedure was performed using as T_y the average value of the annual temperature for this period, i.e., $T_{1871\text{–}1963} = 25.41$°C. The NIST data correspond to the fastest 1-min hurricane speeds at 10 m above ground over open terrain; thus, for this comparison, the coefficients in Eq. (7) assume the values $c_t = c_e = c_z = 1.0$. The results from the proposed simulation method are based on a million samples and are compared with the means and standard deviations obtained from the 999 data points available at each location from the NIST database. These means and standard deviations are conditional on the occurrence of a hurricane event. Figs. 6(a and b) compare the means and standard deviations, respectively, obtained from the NIST data and the proposed model at each considered milepost from the coast of Texas to that of Maine. The 95% confidence intervals for the estimates of the means and standard deviations are also shown, even though those corresponding to the simulated data from the proposed simulation method are not visible at the scale presented in Fig. 6.

Table 4 reports the hurricane wind speed means and standard deviations estimated using the NIST data and the simulated data obtained from the proposed method, as well as the corresponding percentage relative errors, for all the considered mileposts along the US Gulf and Atlantic Coasts. The average relative difference between the simulated and NIST estimates of the hurricane wind speed means is +0.68%, with individual relative differences falling

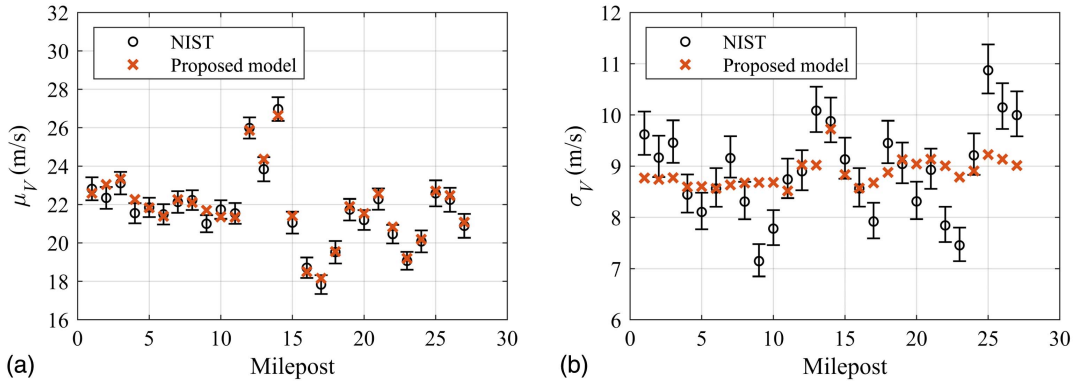

Fig. 6. Comparison of statistics for hurricane wind speed (gradient wind speed corresponding to fastest 1-min hurricane speeds at 10 m above ground over open terrain) obtained from NIST database and from proposed simulation procedure along US Gulf and Atlantic coasts: (a) means; and (b) standard deviations.

between −1.79% and 3.33%. The corresponding root-mean-square error (RMSE) and the modified root-mean-square error (mRMSE) (Peng et al. 2014; Rizzo et al. 2018) for the hurricane wind speed means are equal to 0.33 and 0.00 m/s, respectively. These results indicate that the proposed simulation procedure is able to reproduce very accurately historical data corresponding to hurricane wind speed means along the entire US Gulf and Atlantic Coast region. In fact, the obtained mRMSE value of zero indicates that the simulation estimates of the hurricane wind speed means are always contained within ±2 standard errors from the NIST-based estimates of the means. The difference between the simulated and NIST estimates of the hurricane wind speed standard deviations is +0.07%, with individual relative errors falling between −21.65% and 21.58%. The corresponding RMSE and mRMSE are equal to 0.83 and 0.57 m/s, respectively. The proposed simulation procedure generates estimates of hurricane wind speed standard deviations that are globally representative of the US Gulf and Atlantic coasts; however, it can capture well the effects of geographical differences for the hurricane wind speed means, but not for the hurricane wind speed standard deviations, as observed from Fig. 6.

Table 4. Comparison of hurricane gradient wind speed (fastest 1-min hurricane speed at 10 m above ground over open terrain) means and standard deviations at different mileposts estimated using NIST data and proposed simulation procedure

Milepost number	NIST (m/s)		Proposed model (m/s)		Relative difference (%)	
	μ_V	σ_V	μ_V	σ_V	ε_{μ_V}	ε_{σ_V}
1	22.82	9.62	22.60	8.76	−0.97	−8.92
2	22.35	9.17	23.04	8.66	3.10	−5.52
3	23.11	9.46	23.33	8.79	0.95	−7.08
4	21.55	8.44	22.26	8.53	3.30	1.09
5	21.85	8.11	21.81	8.53	−0.18	5.16
6	21.49	8.56	21.39	8.57	−0.48	0.07
7	22.13	9.16	22.27	8.60	0.62	−6.15
8	22.23	8.31	22.10	8.68	−0.59	4.39
9	21.00	7.15	21.70	8.69	3.33	21.58
10	21.74	7.78	21.35	8.70	−1.79	11.80
11	21.54	8.74	21.34	8.49	−0.94	−2.81
12	25.99	8.9	25.86	9.04	−0.49	1.53
13	23.84	10.08	24.36	9.02	2.20	−10.55
14	26.97	9.88	26.63	9.74	−1.24	−1.45
15	21.06	9.13	21.40	8.85	1.60	−3.08
16	18.71	8.57	18.52	8.59	−1.00	0.22
17	17.83	7.92	18.13	8.66	1.70	9.34
18	19.52	9.45	19.57	8.87	0.28	−6.14
19	21.73	9.04	21.90	9.15	0.79	1.24
20	21.19	8.31	21.54	8.97	1.65	7.99
21	22.28	8.93	22.55	9.12	1.21	2.12
22	20.46	7.84	20.83	8.97	1.82	14.38
23	19.07	7.45	19.19	8.77	0.61	17.76
24	20.08	9.21	20.19	8.92	0.57	−3.13
25	22.58	10.87	22.68	8.52	0.44	−21.65
26	22.25	10.15	22.47	9.10	1.01	−10.30
27	20.89	10.00	21.05	8.99	0.79	−10.10
Average	21.71	8.90	21.85	8.82	0.68	0.07
Minimum	17.83	7.15	18.13	8.49	−1.79	−21.65
Maximum	26.97	10.87	26.63	9.74	3.33	21.58

The second set of data from the design wind speeds given in ASCE 7-16 (ASCE 2016) is used to validate the tail of the hurricane wind speed distributions. In particular, the ASCE 7-16 design wind speeds (also referred to as basic wind speeds) correspond to the 3-s gust wind speeds over open terrain at 10 m above ground at any given location with mean return intervals (MRIs) of 300, 700, 1,700, and 3,000 years, which are used for the design of structures of Risk Categories I through IV, respectively. Thus, the coefficients in Eq. (7) assume the values $c_e = c_z = 1.0$ and $c_t = 1.25$. The design wind speeds in ASCE 7-16 are based on data corresponding to the 1886–1983 period, for which the average yearly SST was calculated as $T_{1886\text{–}1983} = 25.30$°C. Note that the design wind speeds in ASCE 7-16 are obtained from the wind speed distributions, including both hurricane and nonhurricane wind speeds, whereas the wind speeds obtained from the proposed simulation procedure correspond to the hurricane wind speeds only. However, it was also observed that the differences between the two distributions in all the locations considered in this study are negligible for MRIs larger than or equal to 100 years. The design wind speeds obtained from the proposed sampling methodology are based on one million simulations and are obtained as

$$V_{T_{\text{MRI}}} = \text{CDF}^{-1}\left(\frac{T_{\text{MRI}} - 1}{T_{\text{MRI}}}\right) \tag{8}$$

in which $T_{\text{MRI}} = 300$, 700, 1,700, and 3,000 years denotes the MRI of interest; and CDF^{-1} denotes the inverse of the empirical CDF of the generated wind speed data. Table 5 reports the wind speeds corresponding to MRIs of 300, 700, 1,700, and 3,000 years obtained from ASCE 7-16 and from the proposed simulation procedure at each considered milepost from the coast of Texas to that of Maine, as well as the relative differences between the two sets of values. As shown in Table 5, the average relative differences in the design wind speeds over all mileposts are smaller than 1% in absolute

Table 5. Comparison of design wind speeds (base wind speeds corresponding to 3-s gust wind speeds at 10 m above ground over open terrain) from ASCE 7-16 and proposed simulation procedure along US Gulf and Atlantic coasts

Milepost number	ASCE (m/s)				Proposed model (m/s)				Relative difference (%)			
	300	700	1,700	3,000	300	700	1,700	3,000	300	700	1,700	3,000
1	61.24	66.16	69.74	72.42	58.05	62.73	67.60	70.42	−5.20	−5.18	−3.07	−2.76
2	61.69	66.61	70.63	72.87	58.89	63.19	67.66	70.34	−4.53	−5.13	−4.21	−3.47
3	59.9	64.37	68.4	70.19	60.35	64.92	69.65	72.57	0.75	0.85	1.82	3.39
4	58.12	63.48	68.4	70.19	57.87	62.29	66.54	69.53	−0.43	−1.87	−2.72	−0.93
5	67.06	75.1	80.02	82.7	64.04	68.81	73.85	76.89	−4.50	−8.38	−7.71	−7.02
6	66.61	74.21	80.02	81.81	66.46	71.76	76.86	80.24	−0.23	−3.31	−3.95	−1.92
7	65.27	71.53	78.68	81.81	61.70	66.48	71.06	74.22	−5.47	−7.07	−9.69	−9.27
8	56.77	61.24	66.16	68.4	57.63	62.18	66.87	69.51	1.52	1.54	1.08	1.62
9	52.75	58.56	63.48	62.14	53.79	57.99	62.37	65.10	1.97	−0.98	−1.74	4.77
10	50.52	54.54	60.8	62.14	53.13	57.46	61.61	64.60	5.17	5.35	1.34	3.96
11	59.9	64.82	68.4	70.19	57.44	61.86	66.20	69.07	−4.10	−4.56	−3.21	−1.60
12	64.37	69.29	75.1	78.68	64.66	69.59	74.32	77.27	0.45	0.44	−1.04	−1.79
13	71.53	77.34	82.26	85.83	69.66	74.68	79.61	82.83	−2.62	−3.44	−3.22	−3.50
14	69.29	75.55	80.47	83.6	67.92	73.34	78.82	82.39	−1.98	−2.92	−2.05	−1.45
15	61.24	66.61	71.08	75.55	60.24	64.83	69.28	72.35	−1.63	−2.67	−2.53	−4.24
16	53.64	58.12	62.59	66.61	54.21	58.95	63.62	66.97	1.06	1.43	1.64	0.54
17	52.75	58.12	63.93	67.5	53.03	58.04	63.22	66.54	0.53	−0.14	−1.10	−1.42
18	58.56	65.71	70.19	73.76	57.84	63.00	67.99	71.28	−1.22	−4.13	−3.14	−3.36
19	60.35	66.16	69.74	72.87	60.43	65.40	70.27	73.69	0.12	−1.14	0.77	1.12
20	59.9	64.82	67.95	70.19	59.94	64.57	69.52	72.75	0.06	−0.38	2.31	3.65
21	55.43	59.01	63.03	66.16	55.88	60.27	64.50	67.01	0.81	2.13	2.34	1.29
22	49.62	54.09	58.56	60.8	52.34	56.59	61.03	63.72	5.49	4.63	4.22	4.81
23	50.96	55.88	59.9	62.59	51.81	56.28	60.83	63.85	1.68	0.72	1.56	2.02
24	49.62	54.09	58.56	61.24	50.86	55.77	60.03	63.03	2.51	3.11	2.50	2.93
25	54.09	58.12	62.14	64.37	54.67	58.84	63.13	65.67	1.07	1.24	1.60	2.03
26	54.99	59.01	62.59	64.82	57.16	62.36	67.81	70.94	3.94	5.67	8.35	9.44
27	49.17	53.64	57.22	59.46	52.35	57.43	62.10	65.50	6.46	7.06	8.52	10.15
Average	58.35	63.56	68.15	70.7	58.24	62.95	67.64	70.68	0.06	−0.63	−0.42	0.33
Minimum	49.17	53.64	57.22	59.46	50.86	55.77	60.03	63.03	−5.47	−8.38	−9.69	−9.27
Maximum	71.53	77.34	82.26	85.83	69.66	74.68	79.61	82.83	6.46	7.06	8.52	10.15

value for all four risk categories, with minimum and maximum relative differences slightly increasing in absolute values for increasing MRIs. The RMSEs over all considered mileposts for structures corresponding to Risk Categories I–IV are equal to 1.80, 2.55, 2.84, and 3.07 m/s, respectively. It is observed that the proposed simulation procedure can match very well the design wind speeds overall, with only a few locations out of the 27 considered along the US Gulf and Atlantic Coasts where the simulated design wind speeds differ from the ASCE 7-16 design wind speeds by more than 5% (i.e., in 5, 7, 3, and 4 locations for MRIs of 300, 700, 1,700, and 3,000 years, respectively). These locations correspond almost exactly to the locations where higher differences were observed between the NIST-based and the simulated estimates of the hurricane wind speed standard deviations. It is also observed that the average relative differences and the RMSEs of the simulated design wind speed tend to slightly increase for increasing MRIs. Based on the results presented here, it is shown that the proposed simulation approach can capture well both the body and the tail of the hurricane wind speed distributions obtained from historical data for different locations along the US Gulf and Atlantic Coasts.

Hurricane Wind Speed Projections Considering Climate Change: Comparison with Other Existing Models and Design Implications

The proposed simulation procedure is used to develop projected hurricane wind speed distributions under different climate change projections along the US Gulf and Atlantic Coasts. As a further validation of this methodology, its projection results are compared with those obtained from existing methodologies based on a rigorous simulation of hurricane tracks from their formation in the Atlantic Ocean to their landfall on the US Gulf and Atlantic Coasts based on downscaled climate change projections. Specifically, the wind speed projections for the year 2100 in Miami corresponding to the models developed by Cui and Caracoglia (2016) and Pant and Cha (2019) are compared in Fig. 7 to those obtained using

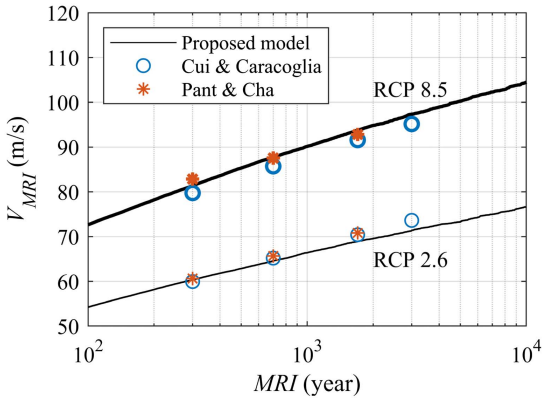

Fig. 7. Comparison of projected hurricane wind speeds (gradient wind speeds corresponding to 3-s gust wind speeds at 10 m above ground over open terrain) for year 2100 in Miami from proposed model, Cui and Caracoglia (2016), and Pant and Cha (2019).

Table 6. Projected increases in design wind speeds (basic wind speeds corresponding to 3-s gust wind speeds at 10 m above ground over open terrain) for year 2060 and scenario RCP 8.5 along US Gulf and Atlantic coasts

Milepost number	300 years		700 years		1,700 years		3,000 years	
	m/s	%	m/s	%	m/s	%	m/s	%
1	11.15	18.21	12.22	18.47	14.35	20.58	15.18	20.97
2	12.25	19.86	13.08	19.64	14.36	20.33	15.62	21.43
3	15.62	26.08	17.04	26.46	19.15	28.00	21.00	29.91
4	14.56	25.06	14.75	23.23	15.45	22.58	17.33	24.69
5	11.61	17.31	9.87	13.14	11.48	14.35	12.90	15.60
6	13.93	20.91	12.69	17.11	13.33	16.66	15.89	19.42
7	11.31	17.33	11.09	15.51	9.74	12.38	10.25	12.53
8	15.35	27.03	16.84	27.49	18.02	27.23	19.33	28.26
9	15.44	29.28	15.30	26.13	15.81	24.91	20.28	32.64
10	16.66	32.97	18.18	33.33	17.67	29.06	19.43	31.27
11	12.24	20.44	13.01	20.07	15.15	22.15	17.11	24.37
12	16.91	26.28	18.15	26.19	18.55	24.70	18.51	23.53
13	13.87	19.39	14.76	19.08	16.37	19.90	16.55	19.28
14	16.76	24.19	17.60	23.30	19.83	24.64	21.04	25.17
15	14.46	23.62	15.15	22.74	16.76	23.58	15.52	20.54
16	14.60	27.22	16.09	27.69	18.00	28.76	17.44	26.18
17	13.77	26.11	14.81	25.48	15.66	24.49	16.20	24.00
18	13.90	23.74	13.38	20.36	15.52	22.11	16.21	21.97
19	16.12	26.71	16.71	25.25	19.43	27.86	20.40	28.00
20	15.60	26.04	16.94	26.14	20.30	29.87	22.07	31.45
21	14.85	26.80	16.87	28.59	18.83	29.87	19.50	29.47
22	11.21	22.60	12.15	22.45	12.77	21.80	14.15	23.28
23	14.36	28.18	15.52	27.78	17.24	28.77	18.44	29.46
24	14.30	28.82	16.00	29.58	17.94	30.64	19.41	31.70
25	14.89	27.53	16.63	28.62	18.37	29.57	19.51	30.30
26	16.39	29.81	19.53	33.09	22.36	35.72	24.81	38.28
27	16.62	33.81	18.83	35.10	21.81	38.12	23.60	39.70
Average	14.40	25.01	15.30	24.52	16.82	25.13	18.06	26.05
Minimum	11.15	17.31	9.87	13.14	9.74	12.38	10.25	12.53
Maximum	16.91	33.81	19.53	35.10	22.36	38.12	24.81	39.70

the proposed model for the climate change scenarios defined by the best-case scenario Representative Concentration Pathway (RCP) 2.6 and the worst case scenario RCP 8.5. The predicted changes in design wind speeds obtained using the proposed model are very close to those provided by the other two models, with a maximum absolute value of the relative differences smaller than 3.0% for the RCP 2.6 scenario (corresponding to a wind speed difference of approximately 2.3 m/s) and smaller than 2.4% for the RCP 8.5 scenario (corresponding to a wind speed difference of approximately 2.2 m/s). It is concluded that the proposed simulation procedure provides projections of wind speed distributions that are consistent with other existing methodologies based on hurricane tracks at a small fraction of their computational cost. For example, the proposed methodology allows to derive the hurricane wind speed distributions based on a million simulations at the 27 different locations and for all 4 climate change scenarios considered in this study in little less than 2 min on an ordinary personal computer [Intel (Santa Clara, California) Core i7-8700 processor, 3.2 GHz, 16 GB RAM].

Finally, the proposed simulation approach is used to estimate the projected wind design speeds under different climate change scenarios at different locations along the US Gulf and Atlantic Coasts. Table 6 reports the projected absolute and relative increases in design wind speeds by year 2060 at each considered milepost from the coast of Texas to that of Maine when considering the RCP 8.5 climate change scenario. These average relative increases in design wind speeds are equal to 25.01%, 24.52%, 25.13%, and 26.05% for structures in Risk Categories I through IV, respectively, with peak relative increases as high as 39.70% near the coast of Maine, where the largest relative increases are expected for all risk categories.

Similar results for other climate change scenarios are not reported here due to space constraints, but the following average relative increases in the design wind speeds are obtained for the four risk categories considered in ASCE 7-16: (1) 14.52%, 14.00%, 14.47%, and 15.27% for RCP 2.6; (2) 18.87%, 18.32%, 18.96%, and 19.82% for RCP 4.5; and (3) 17.87%, 17.39%, 17.97%, and 18.87% for RCP 6.0. Because the design wind force applied on a structure increases quadratically with the design wind speed, these results suggest that, to maintain the same reliability required by the current ASCE 7-16 design code under wind loads, structures with a design life longer than 50 years and located along the US Gulf and Atlantic Coasts should be designed for a larger wind force than that used today, with an increase of at least 30% for RCP 2.6, at least 40% for RCPs 4.5 and 6.0, and between 55% and 59% for RCP 8.5.

Conclusions

This paper proposes a novel and efficient simulation methodology based on historical records to predict hurricane wind speed statistics under different climatological conditions. The developed procedure allows one to simulate hurricane wind speeds at any given location along the US Gulf and Atlantic Coasts by considering the effects of climate change. The newly developed simulation procedure was validated against historical data from NIST and the design wind speeds provided in ASCE 7-16. In addition, the results of the proposed simulation approach were compared with those obtained using other existing procedures requiring the simulation of the full tracks of hurricanes. The obtained hurricane wind speed projections

were found to be consistent (i.e., less than 3.5% absolute relative differences) with those of the other methods while being significantly less computationally expensive (i.e., with a computational time of the order of minutes on an ordinary personal computer). The simulation procedure was used in conjunction with the projection scenarios given in the IPCC's Fifth Assessment Report to simulate hurricane wind speeds corresponding to mean return intervals of 300, 700, 1,700, and 3,000 years (i.e., corresponding to the design wind speeds for buildings belonging to Risk Categories I, II, III, and IV, respectively, in ASCE 7-16) under possible future climatological conditions. The simulation results indicate that climate change could produce significant changes in design wind speeds in the next 40–100 years. In particular, by 2060, the design wind speeds along the US Gulf and Atlantic Coasts are projected to increase between approximately 14% (for Risk Category II under Scenario RCP 2.6) and 26% (for Risk Category IV under Scenario RCP 8.5), corresponding to an average increase of the wind force acting on a structure of between approximately 30% and 59%. Therefore, it is recommended that climate change effects be included in the development of design wind maps for structures with extended design life in future versions of ASCE 7. Finally, whereas the model presented in this study is specifically developed for the US Gulf and Atlantic Coasts, the same methodology can be employed for other hurricane-prone regions worldwide by using the appropriate historical records to fit the numerical values of the parameters used in the present model.

The wind speed model developed in this study provides an invaluable tool for further investigation of climate change effects on the performance of the US built environment and national infrastructure systems. An important aspect that needs to be quantified in future studies is the effect of epistemic uncertainties, e.g., through a sensitivity analysis or a probability bounds analysis of wind speed estimates with respect to the adopted probability distributions, the statistics used to describe such distributions, and the likelihood of different climate scenarios. Another essential research need is the quantification of the effects of the predicted wind force increases on the performance of structural and infrastructural systems, with the resulting implications for future design and building codes for different types of structures, ranging from single-family houses and residential/nonresidential buildings to critical infrastructure components, such as bridges, dams, levees, communication towers, and power plants. Finally, the proposed wind model, used in conjunction with the results of the suggested structural performance studies, could inform the next generation of catastrophe models to predict the effects of climate change in terms of economic and life losses, to assess the resilience of our infrastructure, to quantify the potential societal impact, and, above all, to propose feasible mitigation and adaptation strategies that could be implemented in both the short and long term.

Data Availability Statement

All data, models, and code that support the findings of this study are available from the corresponding author upon reasonable request.

References

Adams, C., E. Hernandez, and J. C. Cato. 2004. "The economic significance of the Gulf of Mexico related to population, income, employment, minerals, fisheries and shipping." *Ocean Coastal Manage.* 47 (11–12): 565–580. https://doi.org/10.1016/j.ocecoaman.2004.12.002.

ASCE. 2016. *Minimum design loads and associated criteria for buildings and other structures*. ASCE/SEI 7. Reston, VA: ASCE.

Barbato, M., F. Petrini, V. U. Unnikrishnan, and M. Ciampoli. 2013. "Performance-based hurricane engineering (PBHE) framework." *Struct. Saf.* 45 (Nov): 24–35. https://doi.org/10.1016/j.strusafe.2013.07.002.

Batts, M. E., E. Simiu, and L. R. Russell. 1980. "Hurricane wind speeds in the United States." *J. Struct. Div.* 106 (10): 2001–2016. https://ascelibrary.org/doi/10.1061/JSDEAG.0005541.

Bjarnadottir, S., Y. Li, and M. G. Stewart. 2011. "A probabilistic-based framework for impact and adaptation assessment of climate change on hurricane damage risks and costs." *Struct. Saf.* 33 (3): 173–185. https://doi.org/10.1016/j.strusafe.2011.02.003.

Bjarnadottir, S., Y. Li, and M. G. Stewart. 2014. "Regional loss estimation due to hurricane wind and hurricane-induced surge considering climate variability." *Struct. Infrastruct. Eng.* 10 (11): 1369–1384. https://doi.org/10.1080/15732479.2013.816973.

Crossett, K., B. Ache, P. Pacheco, and K. Haber. 2013. *National coastal population report: Population trends from 1970 to 2010*. NOAA State of the Coast Rep. Series. Washington, DC: US Dept. of Commerce.

Cui, W., and L. Caracoglia. 2016. "Exploring hurricane wind speed along US Atlantic coast in warming climate and effects on predictions of structural damage and intervention costs." *Eng. Struct.* 122 (Sep): 209–225. https://doi.org/10.1016/j.engstruct.2016.05.003.

Elsner, J. B., S. W. Lewers, J. C. Malmstadt, and T. H. Jagger. 2011. "Estimating contemporary and future wind-damage losses from hurricanes affecting Eglin Air Force Base, Florida." *J. Appl. Meteorol. Climatol.* 50 (7): 1514–1526. https://doi.org/10.1175/2011JAMC2658.1.

Elsner, J. B., J. C. Trepanier, S. E. Strazzo, and T. H. Jagger. 2012. "Sensitivity of limiting hurricane intensity to ocean warmth." *Geophys. Res. Lett.* 39 (17): L17702. https://doi.org/10.1029/2012GL053002.

Emanuel, K. 1999. "Thermodynamic control of hurricane intensity." *Nature* 401 (6754): 665–669. https://doi.org/10.1038/44326.

Emanuel, K. 2011. "Global warming effects on US hurricane damage." *Weather Clim. Soc.* 3 (4): 261–268. https://doi.org/10.1175/WCAS-D-11-00007.1.

Emanuel, K., R. Sundararajan, and J. Williams. 2008. "Hurricanes and global warming: Results from downscaling IPCC AR4 simulations." *Bull. Am. Meteorol. Soc.* 89 (3): 347–367. https://doi.org/10.1175/BAMS-89-3-347.

ESDU (Engineering Sciences Data Unit). 1993. *Strong winds in the atmospheric boundary layer. Part 2: Discrete gust speeds*. ESDU 83045. London: ESDU.

Georgiou, P. N., A. G. Davenport, and B. J. Vickery. 1983. "Design wind speeds in regions dominated by tropical cyclones." *J. Wind Eng. Ind. Aerodyn.* 13 (1–3): 139–152. https://doi.org/10.1016/0167-6105(83)90136-8.

Grinsted, A., J. C. Moore, and S. Jevrejeva. 2013. "Projected Atlantic hurricane surge threat from rising temperatures." *Proc. Nat. Acad. Sci.* 110 (14): 5369–5373. https://doi.org/10.1073/pnas.1209980110.

Hallegatte, S. 2007. "The use of synthetic hurricane tracks in risk analysis and climate change damage assessment." *J. Appl. Meteorol. Climatol.* 46 (11): 1956–1966. https://doi.org/10.1175/2007JAMC1532.1.

Huang, Z., D. V. Rosowsky, and P. R. Sparks. 2001. "Hurricane simulation techniques for the evaluation of wind-speeds and expected insurance losses." *J. Wind Eng. Ind. Aerodyn.* 89 (7–8): 605–617. https://doi.org/10.1016/S0167-6105(01)00061-7.

Jagger, T. H., and J. B. Elsner. 2012. "Hurricane clusters in the vicinity of Florida." *J. Appl. Meteorol. Climatol.* 51 (5): 869–877. https://doi.org/10.1175/JAMC-D-11-0107.1.

Jagger, T. H., J. B. Elsner, and X. Niu. 2001. "A dynamic probability model of hurricane winds in coastal counties of the United States." *J. Appl. Meteorol.* 40 (5): 853–863. https://doi.org/10.1175/1520-0450(2001)040<0853:ADPMOH>2.0.CO;2.

Knutson, T. R., J. L. McBride, J. Chan, K. Emanuel, G. Holland, C. Landsea, I. Held, J. P. Kossin, A. K. Srivastava, and M. Sugi. 2010. "Progress article: Tropical cyclones and climate change." *Nat. Geosci.* 3 (3): 157–163. https://doi.org/10.1038/ngeo779.

Knutson, T. R., J. J. Sirutis, S. T. Garner, I. M. Held, and R. E. Tuleya. 2007. "Simulation of the recent multidecadal increase of Atlantic hurricane activity using an 18-km-grid regional model." *Bull. Am.*

Meteorol. Soc. 88 (10): 1549–1565. https://doi.org/10.1175/BAMS-88-10-1549.

Knutson, T. R., J. J. Sirutis, G. A. Vecchi, S. Garner, M. Zhao, H. S. Kim, M. Bender, R. E. Tuleya, I. M. Held, and G. Villarini. 2013. "Dynamical downscaling projections of twenty-first-century Atlantic hurricane activity: CMIP3 and CMIP5 model-based scenarios." *J. Clim.* 26 (17): 6591–6617. https://doi.org/10.1175/JCLI-D-12-00539.1.

Landsea, C., J. Franklin, and J. Beven. 2015. "The revised Atlantic hurricane database (HURDAT2)." Accessed March 17, 2018. http://www.aoml.noaa.gov/hrd/hurdat/hurdat2.html.

Lee, J. Y., and B. R. Ellingwood. 2017. "A decision model for intergenerational life-cycle risk assessment of civil infrastructure exposed to hurricanes under climate change." *Reliab. Eng. Syst. Saf.* 159 (Mar): 100–107. https://doi.org/10.1016/j.ress.2016.10.022.

Li, Y., and B. R. Ellingwood. 2006. "Hurricane damage to residential construction in the US: Importance of uncertainty modeling in risk assessment." *Eng. Struct.* 28 (7): 1009–1018. https://doi.org/10.1016/j.engstruct.2005.11.005.

Liu, P. L., and A. Der Kiureghian. 1986. "Multivariate distribution models with prescribed marginals and covariances." *Probab. Eng. Mech.* 1 (2): 105–112. https://doi.org/10.1016/0266-8920(86)90033-0.

Lombardo, F. T., and B. M. Ayyub. 2015. "Analysis of Washington, DC, wind and temperature extremes with examination of climate change for engineering applications." *J. Risk Uncertainty Eng. Syst. Part A: Civ. Eng.* 1 (1): 04014005. https://doi.org/10.1061/AJRUA6.0000812.

Malmstadt, J. C., J. B. Elsner, and T. H. Jagger. 2010. "Risk of strong hurricane winds to Florida cities." *J. Appl. Meteorol. Climatol.* 49 (10): 2121–2132. https://doi.org/10.1175/2010JAMC2420.1.

Mudd, L., Y. Wang, C. Letchford, and D. Rosowsky. 2014. "Assessing climate change impact on the US East Coast hurricane hazard: Temperature, frequency, and track." *Nat. Hazards Rev.* 15 (3): 04014001. https://doi.org/10.1061/(ASCE)NH.1527-6996.0000128.

National Hurricane Center. 2018. *Costliest US tropical cyclones tables updated*. NOAA Technical Memorandum NWS NHC-6. Silver Spring, MD: NOAA.

NIST. 2016. "Extreme wind speed data sets: Hurricane wind speeds." Accessed March 17, 2018. http://www.itl.nist.gov/div898/winds/hurricane.htm.

NOAA/OAR/ESRL-PSD. 2015. "NOAA high resolution SST data." Accessed March 25, 2018. http://www.esrl.noaa.gov/psd/.

Oxenyuk, V., S. Gulati, B. M. G. Kibria, and S. Hamid. 2017. "Distribution fits for various parameters in the Florida Public Hurricane Loss model." *J. Mod. Appl. Stat. Methods* 16 (1): 481–497. https://doi.org/10.22237/jmasm/1493598480.

Pant, S., and E. J. Cha. 2018. "Effect of climate change on hurricane damage and loss for residential buildings in Miami-Dade County." *J. Struct. Eng.* 144 (6): 04018057. https://doi.org/10.1061/(ASCE)ST.1943-541X.0002038.

Pant, S., and E. J. Cha. 2019. "Wind and rainfall loss assessment for residential buildings under climate-dependent hurricane scenarios." *Struct. Infrastruct. Eng.* 15 (6): 771–782. https://doi.org/10.1080/15732479.2019.1572199.

Peng, X., L. Yang, E. Gavanski, K. Gurley, and D. Prevatt. 2014. "A comparison of methods to estimate peak wind loads on buildings." *J. Wind Eng. Ind. Aerodyn.* 126 (Mar): 11–23. https://doi.org/10.1016/j.jweia.2013.12.013.

Pielke, R. A., J. Gratz, C. W. Landsea, D. Collins, M. A. Saunders, and R. Musulin. 2008. "Normalized hurricane damage in the United States: 1900–2005." *Nat. Hazards Rev.* 9 (1): 29–42. https://doi.org/10.1061/(ASCE)1527-6988(2008)9:1(29).

Rizzo, F., M. Barbato, and V. Sepe. 2018. "Peak factor statistics of wind effects for hyperbolic paraboloid roofs." *Eng. Struct.* 173 (Oct): 313–330. https://doi.org/10.1016/j.engstruct.2018.06.106.

Soong, T. T. 2004. *Fundamentals of probability and statistics for engineers*. West Sussex, UK: Wiley.

Stocker, T. F., et al. 2013. "Climate change 2013: The physical science basis." In *Proc., Contribution of Working Group I to the 5th Assessment Report of the Intergovernmental Panel on Climate Change*. Cambridge, UK: Cambridge University Press.

Todhunter, I. 2006. *Spherical trigonometry: For the use of colleges and schools*. London: Mamillan and Co.

Unnikrishnan, V. U., and M. Barbato. 2017. "Multihazard interaction effects on the performance of low-rise wood-frame housing in hurricane-prone regions." *J. Struct. Eng.* 143 (8): 04017076. https://doi.org/10.1061/(ASCE)ST.1943-541X.0001797.

Vickery, P. J., F. J. Masters, M. D. Powell, and D. Wadhera. 2009. "Hurricane hazard modeling: The past, present, and future." *J. Wind Eng. Ind. Aerodyn.* 97 (7–8): 392–405. https://doi.org/10.1016/j.jweia.2009.05.005.

Vickery, P. J., P. F. Skerlj, and L. A. Twisdale. 2000. "Simulation of hurricane risk in the US using empirical track model." *J. Struct. Eng.* 126 (10): 1222–1237. https://doi.org/10.1061/(ASCE)0733-9445(2000)126:10(1222).

Webster, P. J., G. J. Holland, J. A. Curry, and H. R. Chang. 2005. "Atmospheric science: Changes in tropical cyclone number, duration, and intensity in a warming environment." *Science* 309 (5742): 1844–1846. https://doi.org/10.1126/science.1116448.

Willoughby, H. E., R. W. R. Darling, and M. E. Rahn. 2006. "Parametric representation of the primary hurricane vortex. Part II: A new family of sectionally continuous profiles." *Mon. Weather Rev.* 134 (4): 1102–1120. https://doi.org/10.1175/MWR3106.1.